

Topology in $SU(2)$ Yang-Mills theory*

B. Allés^{a†}, M. D'Elia^b, A. Di Giacomo^b and R. Kirchner^b

^aDipartimento di Fisica, Sezione Teorica, Università degli Studi di Milano and INFN,
Via Celoria 16, 20133 Milano, Italy.

^bDipartimento di Fisica, Università di Pisa and INFN,
Piazza Torricelli 2, 56126 Pisa, Italy.

New results on the topology of the $SU(2)$ Yang-Mills theory are presented. At zero temperature we obtain the value of the topological susceptibility by using the recently introduced smeared operators as well as a properly renormalized geometric definition. Both determinations are in agreement. At non-zero temperature we study the behaviour of the topological susceptibility across the confinement transition pointing out some qualitative differences with respect to the analogous result for the $SU(3)$ gauge theory.

1. INTRODUCTION

A relevant quantity to understand the breaking of the $U_A(1)$ symmetry in QCD is the topological susceptibility χ in pure Yang-Mills theory [1,2]

$$\chi \equiv \int d^4x \langle 0 | T(Q(x)Q(0)) | 0 \rangle_{\text{quenched}}, \quad (1)$$

where

$$Q(x) = \frac{g^2}{64\pi^2} \epsilon^{\mu\nu\rho\sigma} F_{\mu\nu}^a(x) F_{\rho\sigma}^a(x) \quad (2)$$

is the topological charge density.

The prediction is [1,2]

$$\chi = \frac{f_\pi^2}{2N_f} (m_\eta^2 + m_{\eta'}^2 - 2m_K^2) \approx (180 \text{ MeV})^4 \quad (3)$$

where N_f is the relevant number of flavours. Eq. (3) implies a well defined prescription [1,2] to deal with the $x \rightarrow 0$ singularity in eq. (1).

In [3] χ was evaluated at zero and finite temperature for $SU(3)$ Yang-Mills theory. The value obtained at zero temperature was in agreement with the prediction of Eq. (3). The value of χ at finite temperature displayed a sharp drop beyond the deconfinement transition. Here we give a short review of a similar calculation for the $SU(2)$ gauge

group [4]. In addition we discuss the comparison with the geometric method, and we show that, after a proper renormalization of the latter, the two procedures give consistent results [5].

2. RENORMALIZATIONS

Let $Q_L(x)$ be any definition of the topological charge density on the lattice. The lattice topological susceptibility χ_L is defined as

$$\chi_L \equiv \langle \sum_x Q_L(x) Q_L(0) \rangle. \quad (4)$$

The lattice regulated $Q_L(x)$ is related to the continuum \overline{MS} $Q(x)$ by a finite renormalization [6]

$$Q_L(x) = Z(\beta) Q(x) a^4 + O(a^6) \quad (5)$$

where $\beta \equiv 2N_c/g^2$ in the usual notation.

Since χ_L does not obey in general the prescription [1,2] leading to eq. (3), besides the multiplicative renormalization of eq. (5) there is also an additive renormalization

$$\chi_L = Z(\beta)^2 \chi a^4 + M(\beta) + O(a^6) \quad (6)$$

where $M(\beta)$ contains mixings with operators of dimension ≤ 4 .

In order to extract the physical signal χ from eq. (6), we need a determination of the renormalization constants M and Z . We will determine them using the non-perturbative method of ref. [7,8,3].

*Partially supported by EC Contract CHEX-CT92-0051 and by MURST.

[†]Speaker at the conference.

3. THE MONTE CARLO SIMULATION

We have used Wilson action and the usual heat-bath updating algorithm. The scale $a(\beta)$ was fixed by using the results of ref. [9,10].

3.1. Zero Temperature

The simulation was done on a 16^4 lattice.

We have used various definitions for Q_L . The i -smeared field theoretical $Q_L^{(i)}(x)$ is defined as

$$Q_L^{(i)}(x) = \frac{-1}{2^9 \pi^2} \sum_{\mu\nu\rho\sigma=\pm 1}^{\pm 4} \tilde{\epsilon}_{\mu\nu\rho\sigma} \times \text{Tr} \left(\Pi_{\mu\nu}^{(i)}(x) \Pi_{\rho\sigma}^{(i)}(x) \right). \quad (7)$$

$\Pi_{\mu\nu}^{(i)}$ is the plaquette in the $\mu - \nu$ plane constructed with i -times smeared links $U_\mu^{(i)}(x)$ [11]. We call $M^{(i)}$ and $Z^{(i)}$ the additive and multiplicative renormalization constants for the i -smeared operators. Of course χ must be independent of the choice of the operator Q_L .

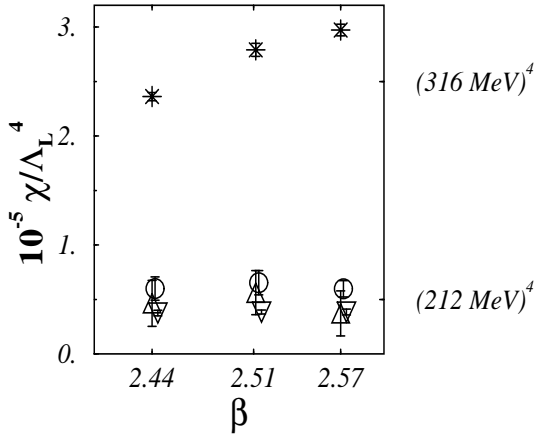


Figure 1. Topological susceptibility at zero temperature.

This is visible in Figure 1, for χ at zero temperature. Up and down-triangles indicate the value of χ as obtained from the 0-smear and 2-smear data respectively. There is good scaling and $(\chi)^{1/4} = (198 \pm 2 \pm 6) \text{ MeV}$, the first error

is statistical and the second comes from the error in Λ_L [9,10].

In Fig. 1 we also report the geometric susceptibility χ_L^g [12,13]. The usual determination is done by identifying $\chi_L^g = \chi a^4$, and claiming that the geometrical susceptibility has no additive renormalization. χ_L^g is shown in Figure 1 by the stars: it is one order of magnitude bigger than the field theoretical determinations and no scaling is observed. By using the same method as for the field theoretical determination, we have measured the multiplicative renormalization Z^g , finding $Z^g = 1$ within errors. At the same time we have determined and subtracted the additive renormalization M^g . This brings down the resulting χ by a factor of 10. The results are shown by the circles in Figure 1 and are in agreement with the field theoretical results. By renormalizing we have eliminated the so-called dislocations.

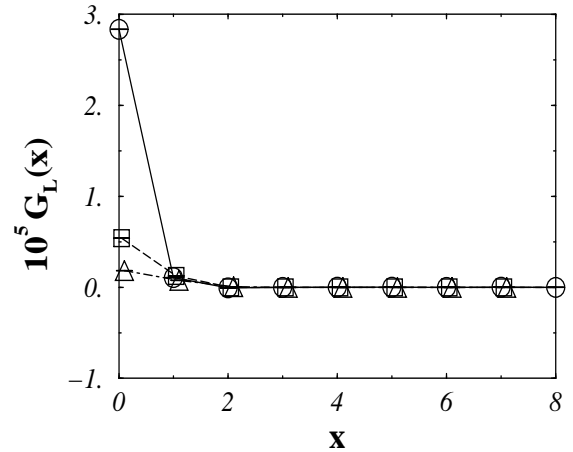


Figure 2. Correlation function for the i -smeared charges at $\beta = 2.57$. The lines are to guide the eye. $i=0,1,2$ correspond to circles, squares and triangles respectively.

To support the necessity of the subtraction of M^g , we have also computed the correlation function

$$G_L(x) \equiv \langle Q_L(x) Q_L(0) \rangle \quad (8)$$

By reflection positivity we expect that $G_L(x) \leq 0$ at $x \neq 0$. Since $\langle Q_L^2 \rangle > 0$, the susceptibility

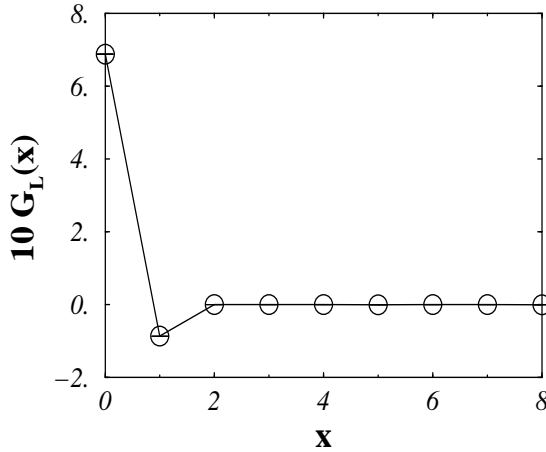


Figure 3. Correlation function for the geometrical charge at $\beta = 2.57$. The line is to guide the eye.

is mainly determined by the singularity at $x = 0$. This correlator, for x lying along a coordinate axis, is shown in Figures 2 for the smeared charges and in Figure 3 for the geometrical charge. The peak at $x = 0$ for the geometric charge is 4 – 5 orders of magnitude larger than for the i -smeared charges, indicating that M^g is much bigger than M^i , $i = 0, 1, 2$, and is $\sim 80\%$ of the observed χ_L .

3.2. Finite Temperature

The simulation was done on a $32^3 \times 8$ lattice. At this size the deconfining transition is located at $\beta_c = 2.5115(40)$ [10] which means that $T_c = 1/(N_t a(\beta_c))$ with N_t the temporal size of the lattice.

The data show again a drop at the transition. However this is less sharp than for the $SU(3)$ case [3,4]. In Figure 4 we show the behaviours for $SU(2)$ and $SU(3)$ of the ratio $\chi(T)/\chi(T = 0)$, where $\chi(T)$ indicates the physical susceptibility at temperature T . The slope for the $SU(3)$ data is steeper. In both cases the data at $T < T_c$ show a constant value consistent with the value at $T = 0$.

We thank Prof. Gerrit Schierholz for providing us with the fortran code for the geometrical charge.

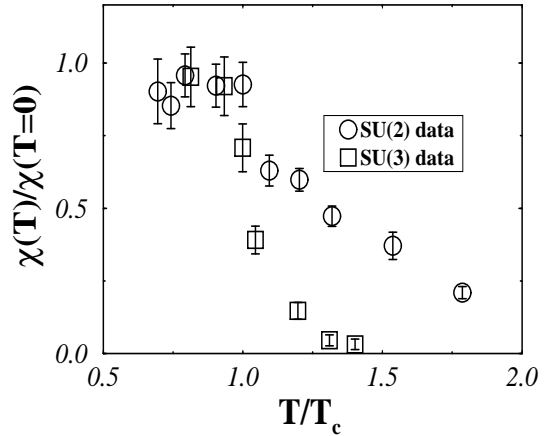


Figure 4. Ratio $\chi(T)/\chi(T = 0)$ for $SU(3)$ and $SU(2)$.

REFERENCES

1. E. Witten, Nucl. Phys. B156 (1979) 269.
2. G. Veneziano, Nucl. Phys. B159 (1979) 213.
3. B. Allés, M. D'Elia, A. Di Giacomo, Nucl. Phys. B494 (1997) 281.
4. B. Allés, M. D'Elia, A. Di Giacomo, hep-lat/9706016, to appear in Phys. Lett. B.
5. B. Allés, M. D'Elia, A. Di Giacomo, R. Kirchner, in preparation.
6. M. Campostrini, A. Di Giacomo, H. Panagopoulos, Phys. Lett. B212 (1988) 206.
7. A. Di Giacomo, E. Vicari, Phys. Lett. B275 (1992) 429.
8. B. Allés, M. Campostrini, A. Di Giacomo, Y. Gündüç, E. Vicari, Phys. Rev. D48 (1993) 2284.
9. J. Engels, F. Karsch, K. Redlich, Nucl. Phys. B435 (1995) 295.
10. J. Fingberg, U. Heller, F. Karsch, Nucl. Phys. B392 (1993) 493.
11. C. Christou, A. Di Giacomo, H. Panagopoulos, E. Vicari, Phys. Rev. D53 (1996) 2619.
12. M. Lüscher, Commun. Math. Phys. 85 (1982) 39.
13. A. Phillips, D. Stone, Commun. Math. Phys. 103 (1986) 599.